PAPER

Dissolution of copper mineral phases in biological fluids and the controlled release of copper ions from mineralized alginate hydrogels

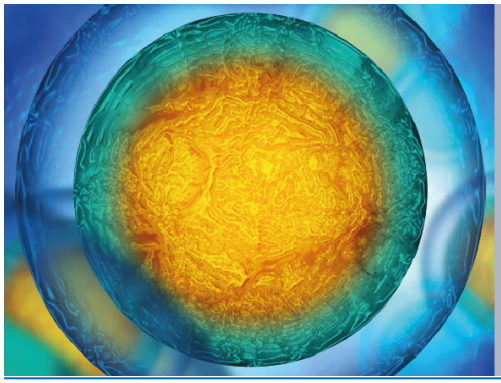

Biomedical Materials

Paper

Dissolution of copper mineral phases in biological fluids and the controlled release of copper ions from mineralized alginate hydrogels

David C Bassett[1], Ivana Madzovska[2], Kai S Beckwith[1], Thor Bernt Melø[1], Bojana Obradovic[2] and Pawel Sikorski[1]

[1] Department of Physics, Norwegian University of Science and Technology, Trondheim, 7491, Norway
[2] Department of Chemical Engineering, Faculty of Technology and Metallurgy, University of Belgrade, Karnegijeva 4, Belgrade, 11000, Serbia

E-mail: david.bassett@ntnu.no

RECEIVED 7 July 2014
REVISED 14 November 2014
ACCEPTED FOR PUBLICATION 14 November 2014
PUBLISHED 29 December 2014

Keywords: bioinorganics, controlled release, alginate, biomineralization, biotechnology

Online supplementary data available from stacks.iop.org/BMM/10/015006/mmedia

Abstract

Here we investigate the dissolution behaviour of copper minerals contained within biocompatible alginate hydrogels. Copper has a number of biological effects and has most recently been evaluated as an alternative to expensive and controversial growth factors for applications in tissue engineering. Precise control and sustained release of copper ions are important due to a narrow therapeutic window of this potentially toxic ion, and alginate would appear to be a good material of choice for this purpose. We found that aqueously insoluble copper minerals could be precipitated during gelling within or mixed into alginate hydrogels in the form of microbeads prior to gelling to serve as depots of copper. These minerals were found to be soluble in a variety of biological fluids relevant to *in vitro* and *in vivo* investigations, and the alginate carrier served as a barrier to diffusion of these ions and therefore offered control over the rate and duration of release (Cu^{2+} release rates observed between 10–750 μMol g^{-1} h^{-1} and duration for up to 32 d). Copper mineral and copper mineralized alginate microbeads were characterized using powder x-ray diffraction, FTIR, thermogravimetric analysis and scanning electron microscopy. Dissolution kinetics were studied based on measurements of copper ion concentrations using colourimetric methods. In addition we characterized the complexes formed between released copper ions and biological fluids by electron paramagnetic spectroscopy which offers an insight into the behaviour of these materials in the body.

1. Introduction

Copper is an essential trace metal that is required by a variety of critical enzymes involved in cellular metabolism [1, 2]. Also, copper has a very narrow therapeutic range, above which it is potently toxic. By virtue of these properties it has found utility as an active ingredient in a wide range of biomedical devices such as contraceptives, (IUD ParaGuard® GyneFix®) [3], anti inflammatory [4], antimicrobial [5], antiviral [6, 7] and anticancer agents [8, 9], as well as enzyme inhibitors [10] and chemical nucleases [11]. In a physiological complex with the bioactive tripeptide glycylhistidyllysine (GHK) it has also been widely studied in the context of wound and scar repair [12]. Besides skin regeneration, copper also mediates cartilage formation, probably through inducing the synthesis of insulin-like growth factor 1 (IGF-1), the major growth factor involved in chondrogenesis [13–15]. In the field of tissue engineering, Cu^{2+} ability to stimulate new blood vessel growth and collagen deposition has recently gained renewed attention to improve vascular integration of synthetic scaffolds [16, 17]. In these experiments, Cu^{2+} was found to work as a substitute or an adjunct to vascular endothelial growth factor (VEGF) offering an interesting and much cheaper alternative to growth factor or cell based approaches to achieve angiogenesis. This stimulatory effect could be due to the fact that copper is essential for the correct cross linking of collagen and elastin fibres which are vital components of vascular tissue [18].

A summary of the biological applications and comparison of the amounts of copper applied in each case is given in table 1. From this table it becomes apparent

Table 1. A summary of the biomedical applications of Cu and an indication of the amounts of Cu applied in each case.

Use	Area or Amount of Cu	Form	Reference
Contraceptive I.U.D.	30–380 mm^{2a}	Elemental Cu	[3, 21, 22]
Anti-inflammatory	IC_{50}: 0.14–86 μM	Complexed Cu^{2+}	[4]
Anti-microbial	IC_{50}: 1.3–4.6 mM	Ionic/Complexed Cu^{2+}	[23]
Anti-viral	16–1600 μM	Ionic Cu^{2+}	[6]
Anti-cancer	Sub to low μM range	Complexed Cu^{2+}	[9]
Enzyme inhibitor	nM range	Complexed Cu^{2+}	[24]
Angiogenesis	35–350 μM	Ionic Cu^{2+}	[16]

[a] Paraguard T 380 A with an exposed copper surface of 380 mm^2 contains a total copper mass of approximately 245 mg [25].

that the metal is applied as either elemental copper, or as ionic Cu^{2+}, present as an aqueously soluble salt (such as copper sulphate) or complexed with an organic molecule. Copper will only be biologically active when it is dissolved and a majority of ionic Cu^{2+} present *in vivo* is complexed with the serum protein ceruloplasmin (a feroxidase enzyme involved in the metabolism of iron), and to a lesser extent with serum albumin [19]. Electron paramagnetic resonance (EPR) spectroscopy has emerged as a powerful tool to investigate the nature of biological copper complexes since Cu^{2+} is paramagnetic. Naturally, a great deal of the literature has focussed on Cu-ceruloplasmin complexes and investigated whether this can be used as a diagnostic tool for diseases such as cancer [20].

From table 1 it can be seen that a wide range (i.e. nM–low mM) of copper is used to bring about strong biological responses. For many of the individual applications the therapeutic range is quite narrow and therefore precise control of the release of Cu^{2+} would appear to be paramount for the biomedical application of this bioactive metal. However, prolonged and controlled release of copper ions within a narrow concentration range or specific flux is a challenge. Alginate represents an exciting material choice for such an application; alginate hydrogels are already used commercially as effective wound and burn dressings by virtue of their high water content and non tissue adhesive properties and they may also be cross linked and therefore functionalized with divalent copper ions [26]. Alginates are a group of linear copolymers consisting of residues of β-D-mannuronic acid (M) and α-L-guluronic acid (G) [27] and may be obtained from both bacterial and marine sources, the latter being the origin of commercially available alginates. The block-like arrangement of G and M residues (M-blocks, G-blocks and MG-blocks) along the polymer chain depend on both the geographical source and seasonal variations [28]. G-blocks, and to a lesser extent regular MG-blocks, may be cross linked by divalent cations (including Cu^{2+}) [29] in aqueous conditions to form a stable hydrogel. The resulting gel properties such as biocompatibility, stability, permeability, mechanical stability and swelling behaviour are significantly affected by the alginate composition and sequential structures and cross-linking ion [30].

Recently we have demonstrated a technique to form alginate microbeads that are mineralized with calcium phosphate or calcium carbonate for application in bone tissue engineering [31]. In the present study we apply the same principle to form alginate microbeads mineralized with copper containing mineral phases, in order to achieve tunable copper releasing properties. We go on to demonstrate controlled release profiles in saline and cell culture medium compared with non-mineralized alginate gels which were cross-linked with copper ions. Furthermore, we use EPR to study the mechanisms responsible for dissolution of copper containing minerals in biological fluids, in particular the formation of complexes between copper ions, amino acids and proteins. We show that alginate preparations containing different copper mineral phases release copper at different rates. This approach gives a new insight into the possible pathways to bioavailable copper and how alginate may be used to as a controlled release matrix for copper ions.

2. Materials and methods

2.1. Materials synthesis

Sodium alginate (either PROTONAL LF 2005 (G content 68% 'High G') or PROTONAL GP 5450 (G content 46% 'Low G'), (FMC Biopolymer, Haugesund, Norway) was dissolved in distilled water at a concentration of 1.9 wt/vol%. All other reactants were purchased from Sigma Aldrich (Oslo, Norway).

To form copper cross-linked alginate beads, alginate solutions with and without mineral precursors (100 mM Na_2HPO_4 or Na_2CO_3) were electrostatically extruded at an applied voltage of 7 kV through a 0.4 mm outer diameter needle (Steadtler Mars Plot 750 PL4 CF) at a constant flow rate of 10 ml h^{-1} using a syringe pump into a continuously stirred 135 mM $CuSO_4$ gelling solution containing 0.9% NaCl. The in-house apparatus used to synthesize beads has previously been described [32]. In order to complete the mineralization process, all samples were aged in the gelling solution for 24 h following bead formation, after which they were washed thoroughly in saline solution prior to further use.

Copper minerals were formed following the aqueous precipitation of Na_2HPO_4 or Na_2CO_3 (both 300 mM) with 135 mM $CuSO_4$ in 0.9% NaCl at room temperature. Precipitates were then washed with deionized water several times using centrifugation prior to further processing.

Table 2. Summary of sample groups.

Code	2% Alginate	Mineral precursor	Mineral addition	Gelling solution[a]
LG	Low G	—	—	135 mM $CuSO_4$
HG	High G	—	—	135 mM $CuSO_4$
LCuC	Low G	100 mM Na_2CO_3	—	135 mM $CuSO_4$
HCuC	High G	100 mM Na_2CO_3	—	135 mM $CuSO_4$
LCuP	Low G	100 mM Na_2HPO_4	—	135 mM $CuSO_4$
HCuP	High G	100 mM Na_2HPO_4	—	135 mM $CuSO_4$
CuC60	High G	—	60 wt% $Cu_2Cl(OH)_3$	50 mM $CaCl_2$
CuC20	High G	—	20 wt% $Cu_2Cl(OH)_3$	50 mM $CaCl_2$
CuC5	High G	—	5 wt% $Cu_2Cl(OH)_3$	50 mM $CaCl_2$
CuP60	High G	—	60 wt% $Cu_3(PO_4)_2.3H_2O$	50 mM $CaCl_2$
CuP20	High G	—	20 wt% $Cu_3(PO_4)_4.3H_2O$	50 mM $CaCl_2$
CuP5	High G	—	5 wt% $Cu_3(PO_4)_4.3H_2O$	50 mM $CaCl_2$

[a] Gelling solutions also contained 0.9% NaCl.

Calcium cross-linked alginate microbeads containing preformed copper mineral (samples CuC60, CuC20, CuC5 and CuP60, CuP20 and CuP5, see table 2) were obtained under the same conditions as copper cross-linked alginate beads by extrusion of High G alginate solution (1.9 wt/vol%) with dispersed copper minerals (atacamite for samples CuCX and copper phosphate for samples CuPX). The copper minerals were produced as explained above and dispersed in the alginate solution by stirring at concentrations of 60, 20 and 5 wt/vol%. These preparations were gelled in 50 mM $CaCl_2$ containing 0.9% NaCl gelling solution. All alginate microbeads were aged in their gelling solutions for a period of 24 h. A summary of the sample group compositions is given in table 2.

2.2. Materials characterization

Samples were dried prior to analysis either under vacuum at room temperature (copper mineral precipitates) or dehydrated in ascending concentrations of ethanol (50–100%) and then critical point dried (alginate samples) using an Emitech K850 CPD (Quorum Technologies, UK). X-ray diffraction (XRD) was performed on dried and crushed samples using a Bruker D8 Focus diffractometer (Bruker AXS Nordic AB, Sweden). Scans were taken in the range of $2\theta = 6$–$60°$, at a step size of 0.02° and dwell time of 1 s step^{-1}. Crystallite sizes were estimated by applying the Scherrer equation to the main diffraction peaks of atacamite (2θ = 16.2°) and tricopper diphosphate trihydrate (2θ = 9.1°). Simultaneous thermogravimetric analysis and differential scanning calorimetry (TGA/DSC—Netzsch STA449C, Netzsch-Gerätebau GmbH, Germany) was performed in the range of 25–1000 °C at a heating rate of 20 °C min^{-1} under an air flow of 80 ml min^{-1}. Fourier transform infrared (FTIR) spectroscopy (Nicolet 8700 FTIR spectrometer, ThermoFisher Scientific, USA) was performed in the range of 600–4000 cm^{-1} at room temperature. An average of 32 scans was taken. Scanning electron microscopy (SEM) was performed on gold coated samples using a Hitachi S-5500 SEM (Hitachi Ltd. Japan) operating at an accelerating voltage of 5 kV.

2.3. Release of Cu^{2+} in DMEM and saline

Alginate microbead samples were retrieved from the gelling solution and thoroughly washed in distilled water and then in 0.9% NaCl solution. 0.25 g of each sample was then placed in a sterile test tube and suspended in 5 ml of either Dulbecco's modified Eagle's medium (DMEM, Invitrogen, Norway) or 0.9% NaCl (saline). All samples were then incubated at 37 °C under static conditions. Following 1, 2, 3, 5, 7, 10 and 14 d incubation 4 ml of the incubation medium was removed and stored and was immediately replaced with fresh medium. This volume was chosen such that accidental removal of alginate microbeads was avoided. Samples were vortexed prior to and following media exchange. Care was taken not to remove beads during the exchange process. All samples were repeated in triplicate.

2.4. Quantification of released Cu^{2+}

Cu^{2+} concentration in release media was detected using a colourimetric assay based on Cu^{2+} complexation with 100 μM 4-(2-Pyridylazo)resorcinol (PAR) [33]. Samples were diluted to within the range of Cu^{2+} detection for 100 μM PAR (i.e. in the range of 0.5–10 μM) using the appropriate incubation medium and absorbance at 514 nm was read using a microplate reader (Tecan Infinite 200 PRO series, Männedorf, Switzerland). Sample Cu^{2+} concentrations were calculated with reference to a standard curve of known concentrations of $CuSO_4$ in both DMEM and saline.

2.5. Studies of mineral dissolution in biologically relevant fluids

In order to determine the dissolution behaviour of the copper minerals in fluids relevant to *in vitro* and *in vivo* biological experimentation, copper minerals were placed in excess and allowed to reach equilibrium with respect to Cu^{2+} ions in the following solutions: 0.9% saline, DMEM (Product #31053 Gibco, Life Technologies), DMEM supplemented with 10% foetal calf serum (FCS), GHK tripeptide (0.4 mM) in phosphate buffered saline (PBS), PBS solutions containing 2 or 3 of the following amino

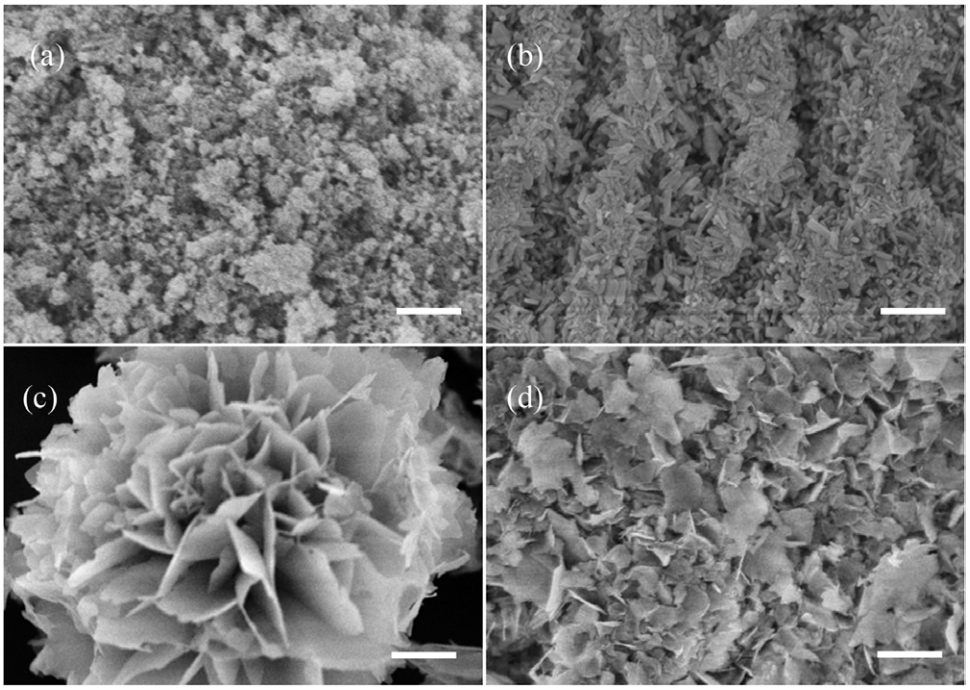

Figure 1. SEM micrographs of (*a*) mineral precipitated in the absence of alginate using Na_2CO_3 precursor (sample CuC), (*b*) surface of alginate microbead sample mineralized using Na_2CO_3 precursor (sample HCuC), (*c*) mineral precipitated in the absence of alginate using Na_2HPO_4 precursor (sample CuP), and (*d*) surface of alginate microbead sample mineralized using Na_2HPO_4 precursor (sample HCuP). Scale bar = 500 nm.

acids at the concentrations found in serum: Glycine (0.4 mM), L-Histidine (0.2 mM) L-Lysine (0.8 mM) and/or Proline (0.4 mM), whole foetal calf serum and 40 mg ml^{-1} bovine serum albumin in PBS. Cu^{2+} concentration was measured using PAR complexation as described in section 2.4. Samples were analysed at 24 h intervals, and once two values at least 24 h apart were recorded to be similar within experimental error, equilibrium was said to have been reached. The pH of all solutions was initially adjusted to 7.4 by the addition of HCl and/or NaOH. All chemicals apart from DMEM were purchased from Sigma Aldrich, Norway.

2.6. EPR spectroscopy

EPR spectroscopy was performed on copper minerals solubilized by the fluids listed in section 2.5 using a JEOL JES-FR30 EPR spectrophotometer (JEOL, Japan). 100 μl samples were placed in a quartz dip cell and spectra were collected between 260–330 mT. The spectra were subjected to analysis using EasySpin in MatLab (version 7.8), using the *chili* program [34], in order to obtain the EPR parameters of the various complexes. In *chili* the stochastic Liouville equation is used to solve the tumbling motion of the molecules and is followed by a fitting routine to obtain the EPR parameters of the sample. Samples were grouped according to similarity by performing principle component analyses of the obtained EPR parameters using MatLab. Each of the g and A tensors extracted from the EPR fits were normalized by z-scoring and analysed using *princomp*. The resulting principal component analysis (PCA) scores for each sample were then plotted along the first and second principle component axes.

3. Results

3.1. Copper alginate bead synthesis and characterization

Two types of alginate were used in this work to create copper containing microbeads, one containing 68% G-blocks (High G) and one containing 46% G-blocks (Low G). Both alginate types rapidly gelled in copper sulphate solution to form non-mineralized hydrogels. Electrostatic assisted dripping of alginate into the gelling bath resulted in formation of spherical gel microbeads with low size variations (Ø 415 ± 28 μm). When aqueously soluble mineral precursors (100 mM Na_2HPO_4 or Na_2CO_3) were added to the alginate solution, precipitates rapidly formed within the gel network upon exposure to copper sulphate solution, resulting in opaque microbeads with well dispersed mineral deposits of the same size and shape as non-mineralized microbeads.

To investigate the role of alginate on the formation of mineral crystals, carbonate and phosphate minerals were formed following the aqueous precipitation of Na_2HPO_4 or Na_2CO_3 with $CuSO_4$ in 0.9% NaCl (samples CuC and CuP – please refer to table 2 for sample descriptions). Minerals formed with carbonate precursors in the absence of alginate appeared poorly crystalline, compared with clearly defined crystals found on the surface of alginate beads (samples LCuC and HCuC, c.f. figures 1(*a*) and 1(*b*)). In contrast crystals formed with phosphate precursors in the alginate microbeads (samples LCuP and HCuP) were slightly smaller and less than alginate free controls (c.f. figures 1(*c*)

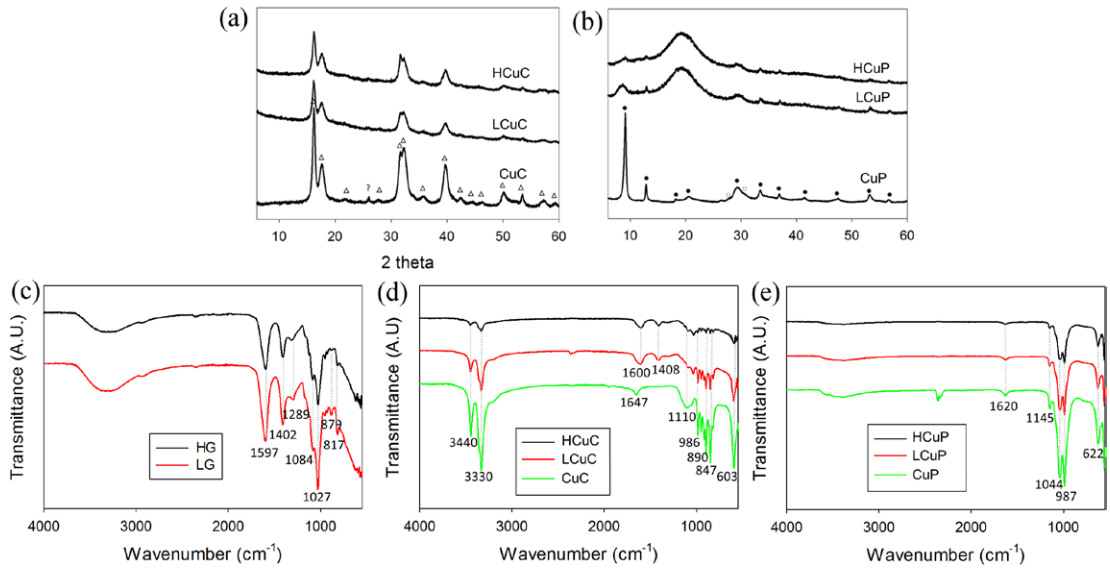

Figure 2. XRD patterns of copper minerals formed from sodium carbonate (*a*) and disodium phosphate (*b*) precursors both in the absence (CuC & CuP) and presence of low and high G containing alginate (H/LCuC & H/LCuP). △ – PDF file 00-025-0269 atacamite ($Cu_2Cl(OH)_3$); ● – PDF file 00-022-0548 tricopper diphosphate trihydrate ($Cu_3(PO_4)_2.3H_2O$); □ – PDF file 00-035—0448 hydroxycupric phosphate heptahydrate ($Cu_8(PO_3OH)_2(PO_4)_4.7H_2O$); ? – unassigned peak. FTIR scans of alginate gelled with copper sulphate (*c*) and also in the presence of sodium carbonate (H/LCuC) (*d*) and disodium phosphate (H/LCuP) (*e*) precursors compared to minerals precipitated in the absence of alginate (CuC & CuP).

and 1(*d*)), as observed by SEM. Figures 2(*a*) and 2(*b*) show the XRD characterization of the mineralized alginate microbeads and pure mineral phases prepared in the absence of the alginate respectively. In all instances, both in the presence and absence of alginate, a carbonate precursor resulted in the formation of atacamite ($Cu_2Cl(OH)_3$), a highly insoluble copper chloride hydroxide, however there was also a minor peak observed in alginate free control samples that could not be assigned. There were no major differences between the XRD patterns for LCuC and HCuC samples. Using a phosphate precursor, tricopper diphosphate trihydrate ($Cu_3(PO_4)_2.3H_2O$) formed under all conditions, along with a minor crystalline phase of hydroxycupric phosphate heptahydrate ($Cu_8(PO_3OH)_2(PO_4)_4.7H_2O$). The mineral phase deposited within the alginate microbeads was poorly crystalline for both LCuP and HCuP samples. The Scherrer equation was used to estimate crystallite size for two mineral phases deposited in the alginate microbeads and prepared in the alginate free conditions (data not shown). For atacamite, crystallite sizes were estimated to be 9.2 ± 0.3 nm, 9.3 ± 0.1 nm and 10.9 ± 0.7 nm for HCuC, LCuC and CuC samples respectively. For tricopper diphosphate trihydrate, the crystallite sizes were estimated to be 6.8 ± 0.4 nm, 4.8 ± 0.4 nm and 20.1 ± 0.3 nm for HCuP, LCuP and CuP samples respectively. It must be noted however, as recently considered for the formation of calcium carbonate mesocrystals [35], that the Scherrer equation underestimates the actual crystallite size in the presence of lattice strain, which is common when minerals are co-precipitated with polymeric additives, and therefore these results should be interpreted with caution. Nevertheless, these results do indicate that there was an effect of alginate on the crystallization of the mineral phase which caused substantial changes to the XRD pattern and the effect was more pronounced for CuP samples. More detailed analyses are required to determine whether there was indeed a reduction in crystallite size and/or increase in lattice strain due to alginate, however this is beyond the scope of this work.

There were little differences in the FTIR spectra recorded for non-mineralized copper cross-linked alginates and agreed well with previously published data [36]. FTIR confirmed the presence of atacamite and a copper phosphate phase within mineralized alginates and no differences in the vibrational spectra were observed between the control mineral phases and those precipitated in the presence of alginate (figures 2(*c*)–(*e*)). Infrared peak assignments are given in table 3. TGA/DSC did not indicate the presence of any amorphous phases (data not shown). TGA was also used to determine the amount of copper present in all preparations (total amount of the mineral phase), and the results are summarized in table 4.

3.2. Controlled release of Cu^{2+} ions

To investigate stability of the mineral phase and release of Cu-ions from mineralized and non-mineralized alginate gels, release kinetics were measured; 0.25 g of alginate microbeads were incubated in 5 ml of release media at 37 °C, and the copper concentration was monitored. In addition, the media was replenished at regular intervals, to simulate a dynamic environment of fluid exchange. The concentration of released copper is given in mM per gram of alginate microbeads. In

Table 3. FTIR peak assignments.

Sample	Band (cm^{-1})	Peak	Ref.
Cu Alginate	1597	$\nu(COO)_{asym}$	[36]
(HG and LG)	1402	$\nu(COO)_{sym}$	
	1289	$\delta(CCH) + \delta(OCH)$	
	1084	$\nu(OCO)$ ring (shoulder)	
	1027	C-O stretch	
	879	C1–H deformation mannuronic acid residues	
	817	Mannuronic acid residues	
CO_3 precursor	3440-3330	$\nu(OH)$	[37, 38]
(CuC, LCuC and	1620–1640	OH bend	
HCuC)	890–990	Cu-O-H bending modes	
PO_4 precursor	1620	OH bend	
(CuP, LCuP and	1145	ν_3 O-P-O asymmetric stretch	[39]
HCuP)	1044	ν_3 O-P-O asymmetric stretch	
	987	ν_1 O-P-O symmetric stretch	
	622	ν_4 O-P-O out of plane bend	

Table 4. Summary of the initial copper content of the various alginate microbead preparations and the percentage of the total amount released in saline and DMEM over 14 d.

Sample	Cu content [wt/wt%][a]	Initial Cu^{2+} conc. [mM^{-1}][b]	Maximum Cu^{2+} release (%) ([mM^{-1}])[c]	
			Saline	DMEM
LG	21.5	5.2	35.5 (1.85)	49.8 (2.59)
HG	21.4	5.2	40.5 (2.11)	53.1 (2.76)
LCuC	45.0	24.2	8.4 (2.03)	52.2 (12.63)
HCuC	39.9	21.4	10.0 (2.14)	48.4 (10.36)
LCuP	30.8	9.8	20.7 (2.03)	58.7 (5.75)
HCuP	30.2	10.5	16.8 (1.76)	64.0 (6.72)
CuC60	44.6	13.7	0.5 (0.07)	62.0 (8.49)
CuC20	30.6	7.3	—	56.0 (4.09)
CuC5	19.6	4.9	—	30.1 (1.47)
CuP60	33.1	13.9	1.3 (0.18)	38.8 (5.39)
CuP20	18.0	6.2	—	43.2 (2.68)
CuP5	7.4	1.8	—	17.6 (0.32)

[a] Cu content of dry samples, calculated from TGA data.
[b] Initial amount of Cu^{2+} present in the release experiments expressed as a concentration. This value represents 100% theoretical release.
[c] Absolute release in mM^{-1} shown in parentheses.

the first instance, release of the copper ions from mineralized and non-mineralized alginate microbeads was measured in 0.9% saline solution. Non-mineralized and mineralized copper alginates released very similar amounts of Cu^{2+} ions (in the range of 7.3–8.5 mM g^{-1}) over 12 d, indicating that the mineral phase had little effect on copper release (figure 3(*a*)). In these samples, the Cu^{2+} released was likely loosely bound to the polymer chains and not directly involved in cross-linking since we did not observe significant bead swelling or disruption over the course of the experiment.

However when the samples were incubated in DMEM, Cu^{2+} was released at a much higher apparent rate for all samples tested (figures 3(*b*) and (*c*)). For non-mineralized alginate microbeads the total amount of Cu^{2+} released was 10.3 ± 0.8 mM g^{-1} and 11.1 ± 1.2 mM g^{-1} for low-G (LG) and high-G (HG) samples respectively; this amount was released within 3 d and the alginate microbeads were completely depleted of releasable Cu^{2+} by this time. Mineralized alginate microbeads released copper into DMEM at a higher rate and release was sustained for a much longer period. LCuC and HCuC samples released 20.3 ± 0.9 mM g^{-1} and 26.3 ± 1.1 mM g^{-1} respectively over the same 3 d time period and went on to release a total of 41.4 ± 1.5 and 50.5 ± 2.1 mM g^{-1} after 14 d of incubation. The higher total release for the LCuC samples was likely due to the greater amount of mineral present in these samples (see table 4). Copper phosphate mineralized samples released Cu^{2+} at a slightly lower rate, releasing 16.5 mM g^{-1} for both LCuP and HCuP samples over 3 d with a total release of 26.8 ± 2.2 mM g^{-1} and 23.1 ± 1.3 mM g^{-1} after 14 d for LCuP and HCuP

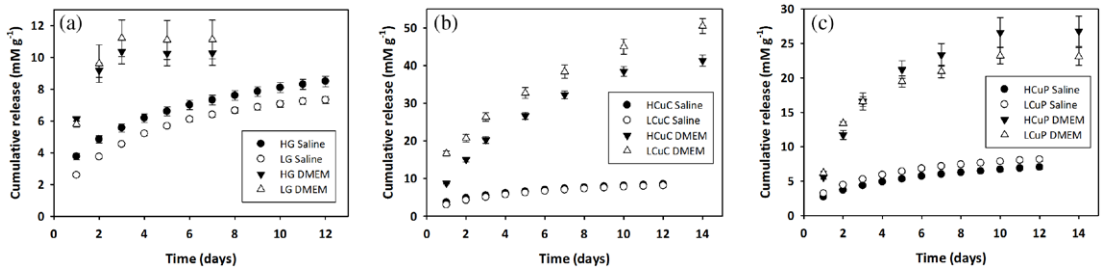

Figure 3. Cu^{2+} release into saline solution and DMEM at 37 °C as measured using PAR complexation comparing non-mineralized copper alginates (*a*), copper alginates mineralized with carbonate precursor (*b*) and phosphate precursor (*c*). Cumulative release is shown as mM of Cu^{2+} per gram of hydrated mineralized or non-mineralized alginate beads. Temperature 37 °C, initial pH 7.4.

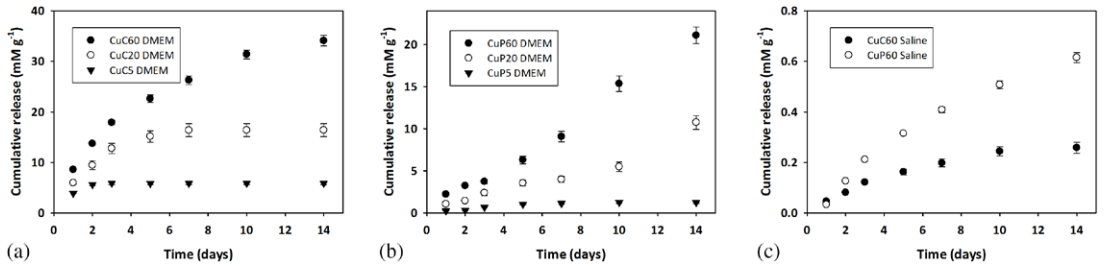

Figure 4. Controlled release of Cu^{2+} ions from calcium cross-linked alginate microbeads containing copper minerals pre-formed with carbonate (*a*) and phosphate (*b*) reagents in DMEM at different loading levels and release in saline solution for 60 wt% mineral samples (*c*). Cumulative release is shown as mM of Cu^{2+} per gram of hydrated alginate beads. Temperature 37 °C, initial pH 7.4.

samples respectively. There was little difference between the release rates for LCuP and HCuP samples, and both contained similar amounts of mineral.

Clearly DMEM increased the solubility of both the copper mineral phases; therefore we sought to examine the effect of incorporating these phases in calcium cross-linked alginate microbeads, such that any Cu^{2+} released originated from the mineral phase. This approach enabled control over the amount of mineral contained within the alginate microbeads, as well as the mineral surface area and resulted in homogeneous mineral distribution within the hydrogel, which should effect the dissolution behaviour. Atacamite and tricopper diphosphate trihydrate prepared by precipitation in the absence of alginate were blended with high G alginate at 5, 20 and 60 wt/vol% proportions before gelling in an aqueous solution of calcium chloride. Cu^{2+} ion release profiles of these samples in saline and DMEM are shown in figure 4. The rate of release was proportional to the amount of mineral present in the sample for both the mineral phases and, as expected, the release rate was much faster in DMEM compared to saline. The initial burst release profile observed previously for copper alginate samples was less apparent for the calcium cross-linked alginate samples, since there were no Cu^{2+} ions loosely bound to the polymer chains. Calcium cross-linked samples released Cu^{2+} at a slower rate than copper cross-linked samples, for example between day 1 and 6 (therefore neglecting the burst release in the first 24 h) LCuC and CuC60 samples that both contained around 45 wt% Cu released Cu^{2+} at a rate of 3.6 mM g^{-1} and 2.9 mM g^{-1} d^{-1} in DMEM respectively. For phosphate containing samples the difference was more pronounced, in the same period LCuP and HCuP samples containing a similar amount of copper to CuP60 samples released 2.5 mM g^{-1} Cu^{2+} per day compared to 1.2 for CuP60. These results indicate that a strong diffusion barrier to the copper ions was formed using calcium to crosslink the alginate. Also, the reduced crystallinity observed with phosphate minerals precipitated in the presence of alginate could have resulted in a greater surface area for dissolution and contributed to a higher rate of Cu^{2+} release. For all mineral containing samples tested atacamite samples released Cu^{2+} ions at a faster rate than copper phosphate samples with an equivalent amount of starting copper content, likely due to a higher solubility of atacamite in DMEM. However, when comparing release rates in saline, copper phosphate containing samples released Cu^{2+} at a faster rate than atacamite containing samples in saline. It must be noted, however, that the release rates in saline were much lower than those achieved in DMEM for both samples (lower by a factor of 19 and 115 for CuP60 and CuC60 respectively).

Release profiles were also measured at shorter time points, shown in figure 5. These results illustrate the initial burst release obtained from copper-crosslinked samples (figure 5(*a*)). Following conditioning of the samples by refreshing the media for 4 d and removing any loosely bound copper, this burst release was greatly reduced and resulted in linear release profiles for calcium cross-linked mineral containing samples (CuP60 and CuC60) (figure 5(*b*)).

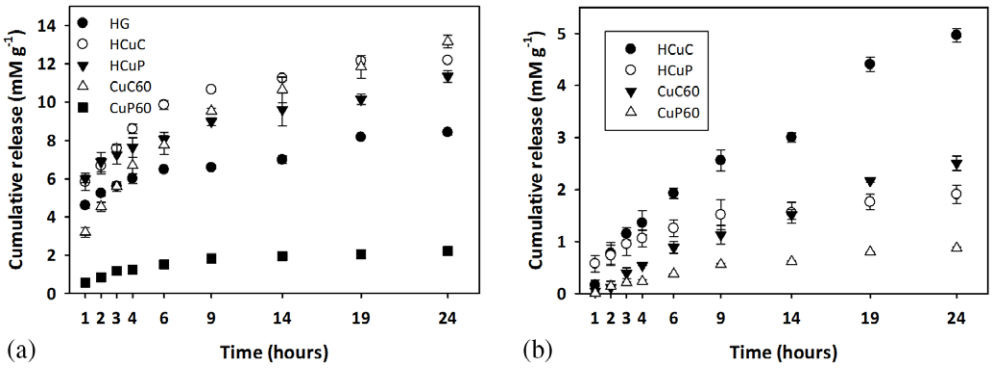

Figure 5. Cu^{2+} release profiles of non-conditioned (*a*) versus samples conditioned for 4 d (*b*) in DMEM. Cumulative release is shown as mM of Cu^{2+} per gram of hydrated alginate microbeads. Temperature 37 °C, initial pH 7.4.

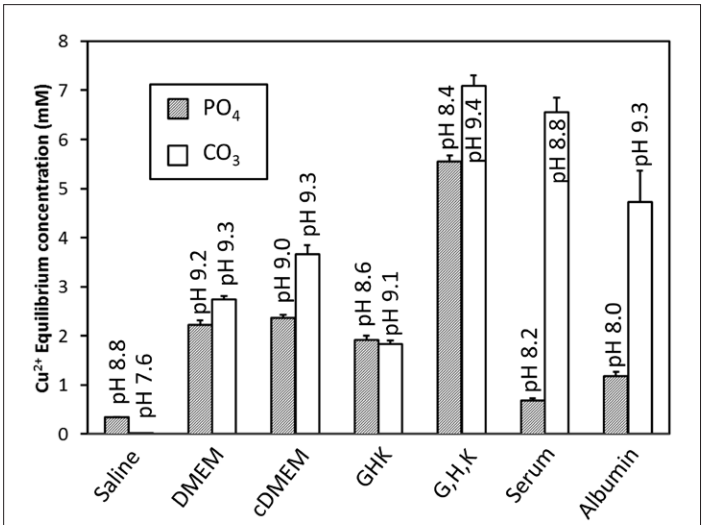

Figure 6. Cu^{2+} equilibrium concentration and pH of copper minerals in biologically relevant media at 37 °C and initial pH of 7.4.

3.3. Solubility of copper minerals in biological fluids

Since we had observed clear differences in release rates obtained for both the different release media and copper mineral phases tested, we sought to determine any differences in mineral solubility in the media tested. It is well established that copper ions may form bioactive complexes with proteins and peptides and we therefore took this as inspiration to investigate the behaviour of atacamite and copper phosphate minerals incubated in a variety of solutions relevant to *in vitro* and *in vivo* biological experimentation. We first determined the solubility of the copper minerals in saline, DMEM, complete DMEM (cDMEM—supplemented with 10% FCS), whole serum, 40 mg ml^{-1} albumin, GHK tripeptide and combinations of the individual amino acids of GHK (i.e. glycine, lysine and histidine—G,H,K) and also combinations substituted with Proline (P). We then used electron parametric resonance (EPR) spectroscopy to investigate the Cu copper complexes formed in these solutions.

Equilibrium Cu^{2+} concentrations and pHs are shown in figure 6. Both mineral phases tested were only sparingly soluble in saline, and solubility was greatly enhanced in DMEM. Atacamite was also much more soluble in whole serum and albumin compared to copper phosphate. This was reflected in differences between DMEM and cDMEM (containing 10% serum) whereby atacamite was found to be more readily solubilized. Both minerals were found to have similar solubilities in GHK tripeptide, which was approximately 3–4 times higher in a solution containing the individual amino acids of GHK (G,H,K) at the concentration present in DMEM, with atacamite slightly more affected than copper phosphate. It should be noted that although the concentration of constituent amino acids was similar for these samples (1.2 versus 1.4 mM) the concentration of the tripeptide as a whole was 3.5 times lower (0.4 mM) which may account for the large differences seen. In all cases there was an increase in pH with copper mineral dissolution, however the increase was not found to be proportional to Cu^{2+} concentration, likely due to differences in the buffering capacity of the solutions tested (figure 6).

3.4. Cu^{2+} complex formation in biological fluids

Electron paramagnetic spectroscopy was used to analyse any complexes that may have formed with

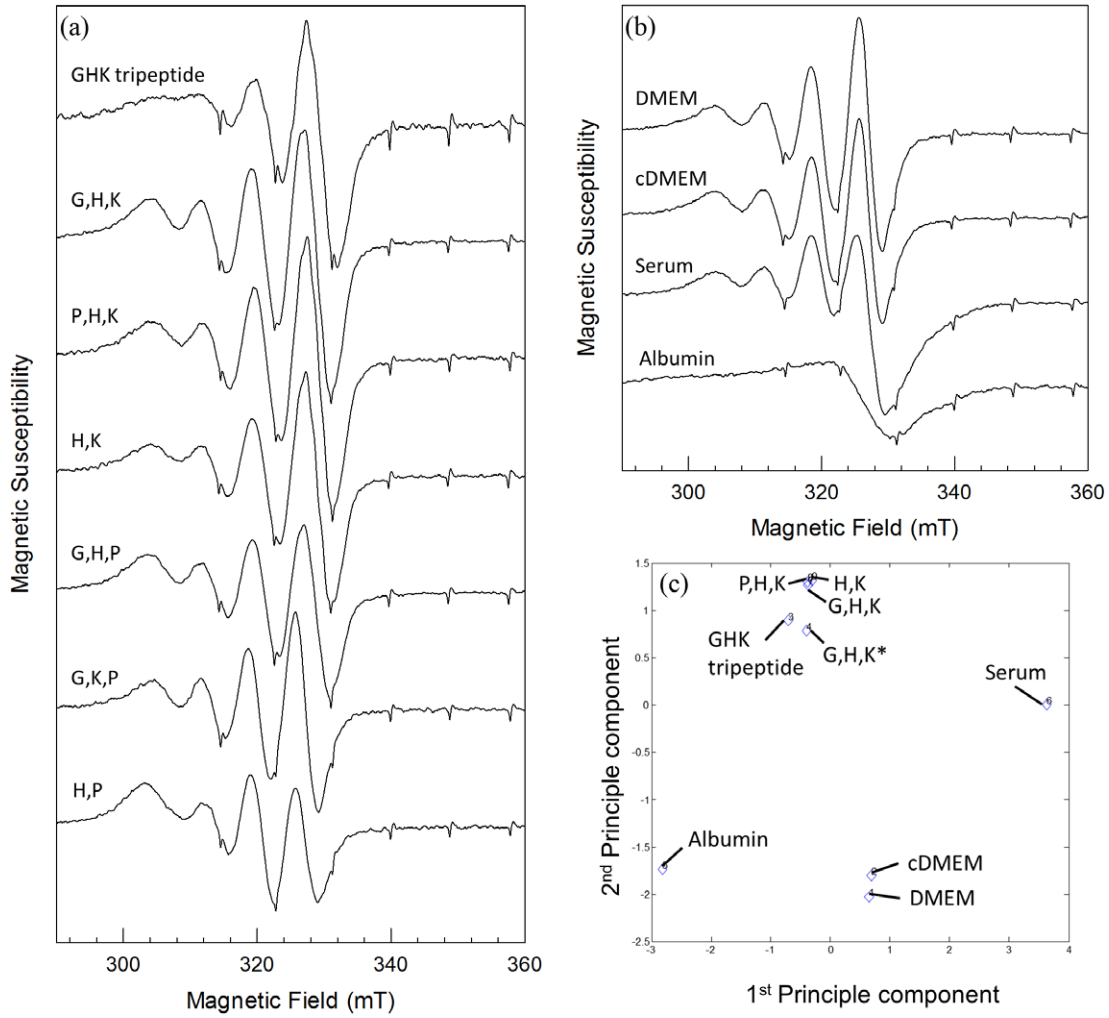

Figure 7. EPR spectra (*a* and *b*) and PCA analysis (*c*) of Cu^{2+} complexes with biological fluids. *denotes the amino acids were present at the equivalent concentration of those present in the GHK tripeptide, otherwise the amino acids were present at the same concentration as found in DMEM.

the solubilizing molecules as a route to characterize the likely mechanisms and state of copper ions in biologically relevant fluids (figure 7(*a*) and (*b*)). The numerical EPR values are shown in supplementary table 1(stacks.iop.org/BMM/10/015006/mmedia). By applying principle component analysis to the modelled spectral parameters of the EPR spectra (figure 7(*c*)) it was found that the individual amino acids G, H and K formed an almost identical complex with Cu^{2+} to that formed with the GHK tripeptide. Indeed it was found that only H and K were required in combination to achieve similar EPR spectra. Different spectra were obtained in DMEM, albumin and serum. Complexes that formed in DMEM were not greatly affected by the addition of serum. The spectrum with albumin alone indicates a very weak interaction with Cu^{2+}. Alternatively the serum albumin could have reduced the Cu^{2+} to Cu^{+}, however it is unlikely a major portion of the ions underwent such a reduction as there was no difference observed in the colour of the solution compared to other samples. The complex in serum showed only certain similarities with the other groups, indicating different or mixed Cu^{2+} ligands.

4. Discussion

4.1. Mineralization and effect of alginate

Copper minerals could be incorporated into alginate hydrogel microbeads through either *in situ* mineralization or by dispersion of preformed mineral and subsequent cross-linking with calcium. These approaches greatly increased the amount of copper that could be contained within the alginate microbeads and also offered a pathway to control the concentration and subsequently the release profiles of Cu^{2+} ions from the alginate hydrogels and extend release from 5 d up to 32 d (release up to 14 d shown). This would appear to be highly relevant for the local delivery of copper ions in a wide range of biomedical devices that require different release amounts (see table 1). It should be noted that the release amounts shown here are representative of a large release, but could easily be tuned by varying not only the composition, as has been demonstrated here, but also the total amount of material applied to a given site.

Copper phosphate crystals formed in the presence of alginate were smaller and less well defined as compared to crystals formed in solution (figure 1) and there

was also a large difference in release profiles compared to calcium cross linked samples made with mineral precipitated in the absence of alginate. However, such a difference in crystallinity and release profiles was not observed for samples made using carbonate precursors, indeed crystals appeared slightly more defined in the presence of alginate. It has previously been shown that alginate and alginate oligomers had a strong influence on crystal growth and polymorph selection of calcium phosphate [31] and calcium carbonate [40], particularly through interaction of the G-blocks in alginate. The mechanisms of crystallization inhibition for these copper minerals appears to be different and warrants further investigation. HCuP and LCuP samples containing *in situ* mineralized CuP released at a much faster rate than CuP60 samples containing a greater amount of pre-formed mineral. This difference may be attributed to the small size and poor crystallinity of *in situ* formed mineral which resulted in a larger surface area and hence a higher solubility. Indeed, even after 32 d, not all of the copper contained in CuP60 samples was released. Additionally, the use of calcium as a crosslinking agent in these samples rendered the microbeads much more stable for extended periods than copper alone, which resulted in bead rupture following copper depletion.

4.2. Solubility and complex formation in biological fluids

We made the intriguing discovery that the solubility of otherwise sparingly aqueously soluble copper salts was greatly enhanced in solutions containing amino acids (e.g. DMEM), GHK peptide, serum or serum albumin. EPR spectroscopy was then used to determine that complexes were formed between copper ions and these biological fluids. Although the ability of amino acids to form soluble complexes with ionic copper is well known [41], the effect on water insoluble copper minerals is, to our knowledge, hitherto unknown. Amino acids, peptides and proteins are essential components of many biological fluids, therefore such a discovery has an important impact on copper bioavailability through many delivery routes. This concept also widens the possibilities of device design in terms of materials selection, since aside from chloride and sulphate salts, copper minerals and metallic copper are largely aqueously insoluble at physiological pH. However, as we have shown, these compounds may behave quite differently in biological fluids. While all fluids tested increased the solubility of both the minerals investigated, the minerals did not behave in the same way; particularly of note is the much higher solubility of atacamite in whole serum and serum albumin solutions compared to copper phosphate. Therefore, there may well be solubility differences between other copper and copper containing minerals in different biological fluids; for example, copper oxide that we have observed has high solubility in DMEM (data not shown) or copper doped calcium phosphates, that have been tested as angiogenesis promoting materials.

Copper is only bioavailable when complexed, and in plasma is thought to be mostly associated with the serum protein ceruloplasmin and to a lesser extent with serum albumin [19]. Cu^{2+} also forms a bioactive complex with the GHK tripeptide which has been shown to be an important factor in wound healing and scar formation [12]. We have shown that analogous complexes may be formed in simple mixtures of amino acids and in DMEM. Indeed in whole serum it would appear that a large proportion of copper ions derived from dissolved mineral were complexed by amino acids and not serum albumin or other serum components. Indeed the EPR spectra obtained for these complexes did not agree with previously published spectra for Cu-ceruloplasmin complexes [42, 43], which indicates that this complex was not formed in our studies. These results therefore indicate an important difference between the *in vitro* and *in vivo* condition of Cu^{2+} ions, which is particularly relevant for cell culture experiments that are generally conducted in serum supplemented DMEM. It is well known that biomaterials in biological systems can bind different components of surrounding environment forming either protein [44] or ion coronas [45]. These coatings affect biomaterial stability, solubility, release profiles and mediate their interaction with cells which all influence the biological effects and toxicity. Our dissolution and complex formation studies highlight the importance of the local environment on copper releasing biomaterials and by taking different approaches to materials design we demonstrate how copper release profiles may be tailored given the different solubilities observed for the different mineral phases in a variety of fluids relevant to *in vitro* and *in vivo* biological experimentation.

Typically, EPR spectra are analysed by extensive modelling to elucidate the detailed interactions between atomic nuclei such as Cu^{2+} and possible ligands [46]. Here, a complementary approach based on principle component analysis (PCA) was used. PCA can greatly simplify complex multivariate datasets by redistributing the data along just a few axes (principle components) that still explain most of the spread in the data. Within EPR spectra analysis, PCA and related methods have mainly been used for denoizing and deconvolution purposes [47]. By applying PCA to the data extracted from the EPR spectra, we uncovered clear sample groupings. Closer inspection of the data extracted from the spectra confirmed that the numerical values for the g and A tensors closely match in the samples grouped by PCA. Thus, we establish numerical spectra fitting followed by PCA as a simple and accessible method to visualize and interpret complex EPR datasets. Naturally, further in-depth analysis can be performed on the same spectra to investigate the details of the ligand structure around the Cu^{2+} ions, but that was not the focus of this work.

4.3. Potential applications and outlook

Bioinorganic agents have emerged as powerful therapies to treat a wide variety of medical disorders

[48–50]. However, the medical application of metallic ions may present specific problems of acute local and systemic toxicity, particularly in the case of copper which has a very narrow therapeutic range for *in vivo* applications (see table 1). Therefore biomaterials which contain metallic ions as bioactive components have to be strictly optimized regarding total metallic content and release rates into the surrounding environment [51]. Here we have shown that by varying the formulation of alginate hydrogels containing copper in ionic and mineral form it is possible to modulate total copper content as well as the release of Cu^{2+}. This approach could have utility in several biomedical applications such as wound dressings and tissue engineering. Bactericidal action due to fast release of Cu^{2+} at high concentration, followed by Cu^{2+} induced skin remodelling and regeneration would potentially enhance the healing process. Taking into account emerging bacterial resistance to antibiotics, Cu-containing biomaterials may represent a promising, highly efficient and cost-effective alternative to standard drug based antimicrobial therapy. In addition, our formulations with linear and sustained release profiles could be suited to tissue engineering applications where controlled and prolonged release of Cu^{2+} is needed in order to promote specific biological responses, such as angiogenesis and chondrogenesis in osteochondral implants or the formation of a microvascular network in every type of tissue graft. In order to avoid risks associated with copper toxicity *in vivo*, but benefit from the effects of Cu^{2+} on specific cell types, such copper-alginate formulations could be used as components of tissue engineering scaffolds to promote tissue regeneration *in vitro* by sustained copper delivery to cultivated cells prior to implantation. These materials could be used in conjunction with other scaffold materials to trigger specific biological responses during cultivation (e.g. expression of cartilaginous genes or stimulation of angiogenesis) to promote tissue maturation and vascular integration upon implantation without recourse for further supplementation with copper. Moreover, such tissue engineering systems could also provide physiologically relevant 3D models for cell biology studies of the effects of Cu^{2+} on individual cells and cell co-cultures as well as novel strategies for stimulation of de novo vascular network formation in engineered tissues *in vitro*.

5. Conclusion

We have shown for the first time that the chemistry of alginate preparations may be modified to allow the simultaneous precipitation of copper containing minerals and cross-linking of alginate hydrogels. Preformed copper minerals could also be incorporated into hydrogels cross-linked with a different divalent cation to allow greater control of copper content and subsequent release profiles. We made the unexpected and intriguing discovery that DMEM enhances the solubility of copper minerals and investigated the solubility of these minerals in a variety of different biological fluids and the complexes that form. This approach demonstrates the flexibility of this material to achieve desired copper release profiles over extended periods of time which may have application in a range of biomedical systems employing copper as a bioactive component.

Acknowledgments

The Research Council of Norway is acknowledged for financial support to DCB and PS through the FRINATEK program (project 214607). The European Cooperation in Science and Technology (COST) framework is acknowledged for support given to IM for a short scientific mission to visit NTNU through the MP1005 NAMABIO action. BO and IM acknowledge the Ministry of Education, Science and Technological Development of the Republic of Serbia (grant III45019).

References

[1] Peña M M O, Lee J and Thiele D J 1999 A delicate balance: homeostatic control of copper uptake and distribution *J. Nutrition* **129** 1251–60
[2] Linder M C and HazeghAzam M 1996 Copper biochemistry and molecular biology *Am. J. Clin. Nutrition* **63** 797S–811S
[3] Zipper J A *et al* 1969 Metallic copper as an intrauterine contraceptive adjunct to T device *Am. J. Obstetrics Gynecol.* **105** 1274–8
[4] Weder J E *et al* 2002 Copper complexes of non-steroidal anti-inflammatory drugs: an opportunity yet to be realized *Coord. Chem. Rev.* **232** 95–126
[5] Ruparelia J P *et al* 2008 Strain specificity in antimicrobial activity of silver and copper nanoparticles *Acta Biomater.* **4** 707–16
[6] Sagripanti J L, Routson L B and Lytle C D 1993 Virus inactivation by copper or iron ions alone and in the presence of peroxide *Appl. Environ. Microbiol.* **59** 4374–6
[7] Sagripanti J L and Lightfoote M M 1996 Cupric and ferric ions inactivate HIV *Aids Res. Human Retroviruses* **12** 333–6
[8] Marzano C *et al* 2009 Copper complexes as anticancer agents *Anti-Cancer Agents Med. Chem.* **9** 185–211
[9] Santini C *et al* 2013 Advances in copper complexes as anticancer agents *Chem. Rev.* **114** 815–62
[10] Mulcahy S P and Meggers E 2010 Organometallics as structural scaffolds for enzyme inhibitor design *Medicinal Organometallic Chemistry* ed G Jaouen and N MetzlerNolte (Berlin: Springer) pp 141–53
[11] Sigman D S, Mazumder A and Perrin D M 1993 Chemical nucleases *Chem. Rev.* **93** 2295–316
[12] Pickart L 2008 The human tri-peptide GHK and tissue remodeling *J. Biomater. Sci.* **19** 969–88
[13] Roughead Z K and Lukaski H C 2003 Inadequate copper intake reduces serum insulin-like growth factor-I and bone strength in growing rats fed graded amounts of copper and zinc *J. Nutrition* **133** 442–8
[14] Wang J G *et al* 2011 Effects of copper on proliferation and autocrine secretion of insulin-like growth factor-1 (IGF-1) and IGF-binding protein-3 (IGFBP-3) in chondrocytes from newborn pigs *in vitro Biol. Trace Elem. Res.* **144** 588–96
[15] Wang J G *et al* 2012 Effect of copper on the expression of IGF-1 from chondrocytes in newborn piglets *in vitro Biol. Trace Elem. Res.* **148** 178–81

[16] Barralet J *et al* 2009 Angiogenesis in calcium phosphate scaffolds by inorganic copper ion release *Tissue Eng.* A **15** 1601–9
[17] Gerard C *et al* 2010 The stimulation of angiogenesis and collagen deposition by copper *Biomaterials* **31** 824–31
[18] Wang S X *et al* 1996 A crosslinked cofactor in lysyl oxidase: redox function for amino acid side chains *Science* **273** 1078–84
[19] Iakovidis I, Delimaris I and Piperakis S M 2011 Copper and its complexes in medicine: a biochemical approach *Mol. Biol. Int.* **2011** 594529
[20] Horn R A *et al* 1979 Electron-spin resonance studies on properties of ceruloplasmin and transferrin in blood from normal human-subjects and cancer-patients *Cancer* **43** 2392–8
[21] Marangoni P, Rodriguez G and Faúndes A 1976 Copper surface area and clinical performance of the copper-bearing T intrauterine device *Contraception* **13** 715–21
[22] Kulier R *et al* 2007 Copper containing, framed intra-uterine devices for contraception *Cochrane Database Syst. Rev.* **4** Cd005347
[23] Dudova B *et al* 2001 Copper complexes with bioactive ligands: I. Antimicrobial activity *Folia Microbiol.* **46** 379–84
[24] Toyota E *et al* 2001 X-ray crystallographic analyses of complexes between bovine β-trypsin and schiff base copper(II) or iron(III) chelates *J. Mol. Biol.* **305** 471–9
[25] ParaGard prescribing information (Sellersville, PA: Teva Women's Health), http://paragard.com/Pdf/ParaGard-PI.pdf (Accessed 4 September 2014)
[26] Grant G T *et al* 1973 Biological interactions between polysaccharides and divalent cations: the egg-box model *FEBS Lett.* **32** 195–8
[27] Draget K I *et al* 1996 Swelling and partial solubilization of alginic acid gel beads in acidic buffer *Carbohydrate Polym.* **29** 209–15
[28] Draget K I, Smidsrød O and Skjåk-Bræk G 2005 Alginates from algae *Biopolymers Online* (Weinheim, Germany: Wiley-VCH Verlag GmbH & Co)
[29] Rui Rodrigues J and Lagoa R 2006 Copper ions binding in Cu-alginate gelation *J. Carbohydrate Chem.* **25** 219–32
[30] Andersen T *et al* 2012 Alginates as biomaterials in tissue engineering *Carbohydrate Chemistry* vol **37** (Cambridge: The Royal Society of Chemistry) pp 227–58 chapter 9
[31] Xie M L *et al* 2010 Alginate-controlled formation of nanoscale calcium carbonate and hydroxyapatite mineral phase within hydrogel networks *Acta Biomater.* **6** 3665–75
[32] Strand B L *et al* 2002 Alginate–polylysine–alginate microcapsules: effect of size reduction on capsule properties *J. Microencapsulation* **19** 615–30
[33] McCall K A and Fierke C A 2000 Colorimetric and fluorimetric assays to quantitate micromolar concentrations of transition metals *Anal. Biochem.* **284** 307–15
[34] Stoll S and Schweiger A 2006 EasySpin, a comprehensive software package for spectral simulation and analysis in EPR *J. Magn. Reson.* **178** 42–55
[35] Kim Y-Y *et al* 2014 A critical analysis of calcium carbonate mesocrystals *Nat. Commun.* **5** 4341
[36] Papageorgiou S K *et al* 2010 Metal-carboxylate interactions in metal-alginate complexes studied with FTIR spectroscopy *Carbohydrate Res.* **345** 469–73
[37] Frost R L *et al* 2002 Raman spectroscopy of the basic copper chloride minerals atacamite and paratacamite: implications for the study of copper, brass and bronze objects of archaeological significance *J. Raman Spectrosc.* **33** 801–6
[38] Malvault J Y *et al* 1995 Cathodic reduction and infrared reflectance spectroscopy of basic copper(ii) salts on copper substrate *J. Appl. Electrochem.* **25** 841–5
[39] Farmer V C 1974 *The Infrared Spectra of Minerals* (London: Mineralogical Society)
[40] Olderoy M O *et al* 2009 Growth and nucleation of calcium carbonate vaterite crystals in presence of alginate *Crystal Growth Des.* **9** 5176–83
[41] Graddon D P and Munday L 1961 Some properties of copper(II) α-amino-acid chelates: A study of solubilities, visible region and infra-red spectra in relation to crystal structure *J. Inorg. Nucl. Chem.* **23** 231–44
[42] Andreasson L E and Vanngard T 1970 Evidence of a specific copper II in human ceruloplasmin as a binding site for inhibitory anions *Biochim. Biophys. Acta* **200** 247–57
[43] Mailer C *et al* 1974 Identity of paramagnetic element found in increased concentrations in plasma of cancer-patients and its relationship to other pathological processes *Cancer Res.* **34** 637–42
[44] Lundqvist M *et al* 2008 Nanoparticle size and surface properties determine the protein corona with possible implications for biological impacts *Proc. Natl Acad. Sci. USA* **105** 14265–70
[45] Ehrenberg M S *et al* 2009 The influence of protein adsorption on nanoparticle association with cultured endothelial cells *Biomaterials* **30** 603–10
[46] Goodman B A, McPhail D B and Powell H K J 1981 Electron spin resonance study of copper(II)-amino-acid complexes: evidence for cis and trans isomers and the structures of copper(II)-histidinate complexes in aqueous solution *J. Chem. Soc. Dalton Trans.* **3** 822–7
[47] De Volder P *et al* 1991 Maximum likelihood common factor analysis in Auger electron spectroscopy *Surf. Interface Anal.* **17** 363–72
[48] Thompson K H and Orvig C 2003 Boon and bane of metal ions in medicine *Science* **300** 936–9
[49] Bakhtiar R and Ochiai E I 1999 Pharmacological applications of inorganic complexes *Gen. Pharmacol.* **32** 525–40
[50] Habibovic P and Barralet J E 2011 Bioinorganics and biomaterials: bone repair *Acta Biomater.* **7** 3013–26
[51] Mourino V, Cattalini J P and Boccaccini A R 2012 Metallic ions as therapeutic agents in tissue engineering scaffolds: an overview of their biological applications and strategies for new developments *J. R. Soc. Interface* **9** 401–19